



A transient three-dimensional heat transfer model of the human body [☆]

M.S. Ferreira ^a, J.I. Yanagihara ^{b,*}

^a Department of Mechanical Engineering, FEI (Fundação Educacional Inaciana), São Bernardo do Campo, Brazil

^b Department of Mechanical Engineering, Polytechnic School, University of São Paulo, Av. Prof. Mello Moraes, 2231, 05508-900, São Paulo, SP, Brazil

ARTICLE INFO

Available online 16 April 2009

Keywords:

Human body thermal model
Human thermal system
Bio-heat transfer
Thermoregulation
Thermal comfort

ABSTRACT

The objective of this work is to develop an improved model of the human thermal system. The features included are important to solve real problems: 3D heat conduction, the use of elliptical cylinders to adequately approximate body geometry, the careful representation of tissues and important organs, and the flexibility of the computational implementation. Focus is on the passive system, which is composed by 15 cylindrical elements and it includes heat transfer between large arteries and veins. The results of thermal neutrality and transient simulations are in excellent agreement with experimental data, indicating that the model represents adequately the behavior of the human thermal system.

© 2009 Elsevier Ltd. All rights reserved.

1. Introduction

The human thermal system is composed of the thermoregulatory and the passive system. The former is related to the physiological responses to changes in the thermal environment or activity level: vasodilatation or constriction, shivering, and sweating. The later includes heat conduction inside the body, heat transfer by convection because of flowing blood, and heat transfer between the body and the environment.

Several models of the human thermal system have been developed. One cylinder models – Fanger [1], Gagge et al. [2], Ferreira and Yanagihara [3] – can be used to predict global thermal comfort conditions, to investigate the sensitivity of a simulation to some parameters, and to test temperature regulatory strategies. All of them incorporate basic features, such as heat conduction in tissues, heat transfer between blood and tissue, metabolic heat generation, and heat transfer by convection, radiation, evaporation of sweat, and through respiration. Multi-segmented models – Wissler [4,5], Gordon et al. [6], Tikuisis et al. [7], Werner [8], Takemori et al. [9], Fiala et al. [10,11], Huizenga et al. [12], Tanabe et al. [13], Salloum et al. [14], Wan and Fan [15], and Al-Othmani et al. [16] – have more advanced applications, including evaluation of local thermal comfort and simulation of human physiological responses to cold water immersion. Werner and Buse [17] and Takemori et al. [9] considered 3D heat conduction.

Thermal comfort evaluation requires the simulation of asymmetric boundary conditions, which occur when there are sources of thermal radiation, air currents, or contact between part of the human body and a solid object. The aforementioned boundary conditions require the use of a 3D model, i.e., to consider 3D heat conduction inside the human body. Body geometry is usually represented by circular cylinders, each one representing a segment of the body. The use of circular cylinders results in elements with unrealistic lengths, feature incompatible with a 3D

model. In this study, cylinders with elliptical cross section were used in order to achieve a better geometric representation of the human body.

2. Model description

2.1. Geometric and anatomic model

The global data of the anatomic model used [17] are height 1.76 m, weight 67 kg, surface 1.8 m², and volume 6.27×10^{-2} m³. The human body was divided in 15 cylinders representing the head, neck, trunk, arms, forearms, hands, thighs, legs, and feet. The comparison presented in Table 1 shows that the use of cylinders with elliptical cross sections generates a model with realistic dimensions. The hand and trunk lengths in the model of Takemori et al. [9] are exaggerated because of their extensive superficial area. In the present model, the ellipse eccentricity accounts for this large area. The height obtained is 1.77 m.

The tissues considered were: skin, fat, muscle, bone, brain, viscera, lung, and heart. The choice was not arbitrary: (a) the skin was considered because its blood flow is variable, and it is dictated by the thermoregulatory system; (b) the fat was considered because it has the smallest thermal conductivity among the human tissues, behaving as a thermal insulation; (c) the muscle, because its blood flow and metabolism vary according to the physical activity and shivering level; (d) the bone, because its thermal properties and blood flow are very different from other tissues. Its thermal conductivity is the biggest and its specific heat, the smallest; (e) the lung, because its blood flow is approximately equal to the cardiac output and it has a small density; (f) the heart, because it has a high metabolic heat generation; (g) the brain, because it has a high metabolic heat generation and blood flow. Besides that, its temperature is considered to be an input to the regulatory system (the temperature of the hypothalamus pre-optic area to be more specific); and finally (h) the viscera, a homogeneous mixture of the following tissues – liver, kidney, stomach, gut, pancreas, spleen, bladder, and connective tissue – were considered because of their high metabolic heat generation and blood

[☆] Communicated by W.J. Minkowycz.

* Corresponding author.

Nomenclature

a	major ellipse semi-axis (cm)
b	minor ellipse semi-axis (cm)
c	specific heat ($\text{J kg}^{-1} \text{K}^{-1}$)
f_{cl}	ratio between the surface area of the clothed segment and the nude one
h	combined heat transfer coefficient ($\text{W m}^{-2} \text{K}^{-1}$)
h_{av}	heat transfer coefficient between one big artery and vein ($\text{W K}^{-1} \text{pair}^{-1}$)
h_c	convective heat transfer coefficient ($\text{W m}^{-2} \text{K}^{-1}$)
h_e	evaporative heat transfer coefficient ($\text{W m}^{-2} \text{Pa}^{-1}$)
h_r	radiative heat transfer coefficient ($\text{W m}^{-2} \text{K}^{-1}$)
k	thermal conductivity ($\text{W m}^{-1} \text{K}^{-1}$)
L	cylinder length (cm)
m	mass (kg)
t	time (s)
v	air speed (m s^{-1})
w	skin wettedness
x	spatial coordinate (m), is equal to $\xi \cdot a \cdot \cos \eta$
y	spatial coordinate (m), is equal to $\xi \cdot b \cdot \sin \eta$
z	spatial coordinate (m), is equal to γ
A_s	superficial area (m^2)
CR	heat transfer flux by convection and radiation (W m^{-2})
E	heat transfer flux by evaporation (W m^{-2})
H_{av}	heat transfer coefficient between artery and vein reservoirs (W K^{-1})
J	Jacobian (m^2), is given by $x_\xi \cdot y_\eta - y_\xi \cdot x_\eta$
K	thermoregulatory system constant
M	metabolic heat generation per unit volume (W m^{-3})
P_w	partial water vapor pressure at the environment temperature (Pa)
$P_{w,sk}$	water vapor pressure at the skin surface temperature (Pa)
Q	heat lost (W)
R_{cl}	thermal resistance of cloth ($\text{W}^{-1} \text{m}^2 \text{K}$)
$R_{e,cl}$	resistance to evaporation imposed by clothes ($\text{W}^{-1} \text{m}^2 \text{Pa}$)
T	temperature ($^\circ\text{C}$)
W	blood flow rate ($\text{m}^3 \text{s}^{-1}$)

Greek symbols

Δ	variation
γ	spatial coordinate in the transformed space
η	spatial coordinate in the transformed space
ξ	spatial coordinate in the transformed space
ρ	tissue density (kg m^{-3})
ϕ	relative humidity of the air
ω_{bl}	tissue blood perfusion rate ($\text{m}^3 \text{m}^{-3} \text{s}^{-1}$)

Subscripts

0	reference or set-point
ar	arterial
bl	blood
hy	hypothalamus
i	i th segment
in	
o	operative
re	rectal
sk	skin
sh	shivering

sw	sweat
ty	tympanic
ve	venous
w	water vapor

flow. Mean viscera and brain temperatures can represent rectal and hypothalamic temperature, respectively. The tissues thermal properties and physiological parameters used are presented in Table 2. The data were taken from Werner and Buse [17]. The arrangement of layers (Figs. 1–4) was based on human body cross-section photos [18]. The distribution in the neck is similar to the arm, and it is not represented here.

2.2. Heat transfer by conduction inside the body

The heat conduction equation with constant density and specific heat is given by:

$$\rho \cdot c \cdot (T)_t = (k \cdot T_x)_x + (k \cdot T_y)_y + (k \cdot T_z)_z + M \quad (1)$$

where ρ is the tissue density, c is the specific heat, T is the temperature, k is the thermal conductivity; x, y, z , and t denote derivation with respect to x, y, z , and time; M is the internal heat generation.

The numerical solution of Eq. (1) can be achieved using a coordinate transformation [19], which transforms an elliptical cylinder in the Cartesian space into a parallelepiped in the new coordinate system, with axes ξ, η , and γ . Eq. (1), rewritten in the new coordinate system, is given by:

$$J \cdot \rho \cdot c \cdot T_t = \left[\frac{k \cdot (x_\eta^2 + y_\eta^2)}{J} \cdot T_\xi - \frac{k \cdot (x_\xi \cdot x_\eta + y_\xi \cdot y_\eta)}{J} \cdot T_\eta \right]_{\xi} \quad (2)$$

$$+ \left[\frac{k \cdot (x_\xi^2 + y_\xi^2)}{J} \cdot T_\xi - \frac{k \cdot (x_\xi \cdot x_\eta + y_\xi \cdot y_\eta)}{J} \cdot T_\eta \right]_{\xi}$$

$$+ J \cdot [k \cdot T_\gamma]_\gamma + J \cdot M$$

where J is the Jacobian of the transformation.

Assuming symmetrical and uniform environments the heat transfer by convection and radiation in each element can be calculated by:

$$CR = \frac{T_{sk} - T_o}{R_{cl} + \frac{1}{f_{cl} \cdot h}} \quad (3)$$

where CR is the heat transfer by convection and radiation, T_{sk} and T_o are the superficial skin temperature and the operative temperature, R_{cl} is the thermal resistance of the cloth, f_{cl} is the ratio between the surface area of the clothed segment and the nude one, and h is the combined heat transfer (convection + radiation) coefficient in the element. The heat transfer coefficients were taken from the experiments of Dear et al. [20]. The evaporative coefficient (Eq. (7)) was calculated from the convective coefficient using the analogy between heat and mass transfer. The coefficients are presented in Table 3 and compared with experimental data. The cloth was modeled as an additional heat and mass transfer resistance [21].

The heat transfer by evaporation at the surface of each element can be calculated by:

$$E = w \cdot \frac{P_{w,sk} - \phi_a \cdot P_{w,a}}{R_{e,cl} + \frac{1}{f_{cl} \cdot h_e}} \quad (4)$$

where E is the heat transferred by evaporation, $P_{w,sk}$ is the water vapor pressure at the skin surface temperature, w is the skin wettedness (varies from 0.06, when there is only water diffusion, to 1.0, when the skin is completely wetted by sweat), ϕ is the relative humidity of the air;

Table 1
Comparison between dimensions of geometric models.

Element	Present model					Takemori et al. [9]	
	V/cm ³	A _s /cm ²	L/cm	2a/cm	2b/cm	L/cm	D/cm
Head	3542	1135	20	13.1	17.3	20.7	14.6
Neck	850	294	8	12.8	10.5	8.3	11.4
Trunk	34,758	5985	60	35.7	20.7	79.8	26.0
Arm	1766	831	31	8.1	9.0	35.3	9.0
Forearm	988	601	28	7.9	5.7	29.2	7.4
Hand	500	450	19	10.9	3.1	30.0	4.6
Thigh	5224	1701	44	11.9	12.7	35.2	13.4
Leg	2317	1080	40	8.3	8.9	37.9	8.6
Foot	980	630	26	10.2	4.7	24.1	7.2

Where *L* is the length, *a* is the major and *b* the minor ellipse semi-axis, *V* is the volume, *A_s* is the superficial area and *D* the is cylinder diameter.

P_w is the partial water vapor pressure at the environment temperature, *R_{e,cl}* is the resistance to evaporation imposed by the clothes, and *h_e* is the evaporative heat transfer coefficient in the element.

The respiratory heat loss was calculated using the model proposed by Fanger [1]. This heat loss was modeled as a sink of heat and it was divided according to [10]: 45% and 25% to the head and neck muscles, and 30% to the lung.

2.3. Heat transfer between blood and tissue

For small vessels that can be treated as part of a continuum, the model of Chen [24] without the convective term and the eddy conductivity can be applied. The model is similar to that proposed by Pennes [25], the difference is that arterial blood temperature depends on the position inside the tissue and is not equal to the body core temperature. The new term, the heat transfer between blood and tissue in the small vessels, to be added to Eq. (2) is:

$$J \cdot \omega_{bl} \cdot \rho_{bl} \cdot c_{bl} \cdot (T_{ar,i} - T) \tag{5}$$

where ω_{bl} is the tissue blood perfusion rate, ρ_{bl} is the blood density, c_{bl} is the blood specific heat, and $T_{ar,i}$ is the temperature of the arterial blood that supplies the small vessels in the segment *i*.

The big vessels can be modeled as proposed by Wissler [5], using two reservoirs, one of arterial blood and the other of venous blood. The head, neck, arms, forearms, hands, thighs, legs, and feet have two reservoirs. Applying a heat balance to each reservoir, the differential equation, Eqs. (6) and (7), that describes the arterial and venous blood temperature variations is obtained. Only one reservoir was considered in the trunk. The equation is similar to Eq. (7), but with $H_{av} = 0$ and

Table 2
Properties and parameters used in the model.

Tissue	$\rho/$ (kg m ⁻³)	$c/$ (J kg ⁻¹ K ⁻¹)	$k/$ (W m ⁻¹ K ⁻¹)	BM/ (W m ⁻³)	BBF × 10 ⁶ / (m ³ m ⁻³ s ⁻¹)
Skin	1085	3680	0.47	368	362
Fat	920	2300	0.21	368	77
Muscle	1085	3800	0.51	684	543
Bone	1357	1700	0.75	368	0
Brain	1080	3850	0.49	9472	9000
Lung	560	3520	0.28	339	41,301
Heart	1080	3550	0.47	24,128	14,400
Viscera	1080	3504	0.49	3852	8925
Blood	1059	3850	–	0	–

ρ is the tissue density, *c* the specific heat, *k* the thermal conductivity, BM is the basal metabolism, and BBF is the tissue basal blood perfusion rate.

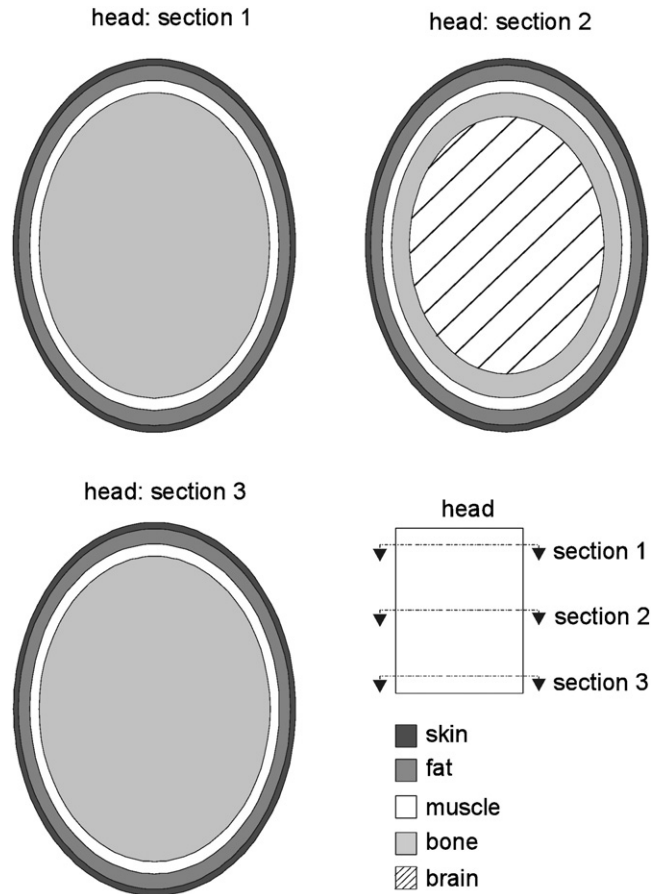


Fig. 1. Distribution of layers in the head.

three blood streams coming from the neck, upper and lower limbs, instead of one.

$$m_{ar,i} \cdot c_{bl} \cdot [T_{ar,i}]_t = \rho_{bl} \cdot c_{bl} \cdot W_{ar,in} \cdot (T_{ar,in} - T_{ar,i}) + H_{av,i} \cdot (T_{ve,i} - T_{ar,i}) \tag{6}$$

$$m_{ve,i} \cdot c_{bl} \cdot [T_{ve,i}]_t = \rho_{bl} \cdot c_{bl} \cdot W_{ve,in} \cdot (T_{ve,in} - T_{ve,i}) + H_{av,i} \cdot (T_{ar,i} - T_{ve,i}) \tag{7}$$

$$+ \int_V \rho_{bl} \cdot c_{bl} \cdot \omega_{bl} \cdot (T - T_{ve,i}) dV$$

where $m_{ar,i}$ and $m_{ve,i}$ are the masses of blood in the arterial and venous reservoirs of segment *i*, respectively; $W_{ar,in}$ and $W_{ve,in}$ are the total

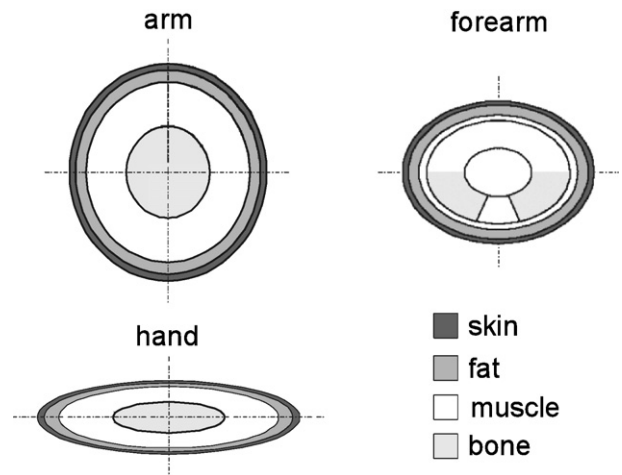


Fig. 2. Distribution of layers in the upper limbs.

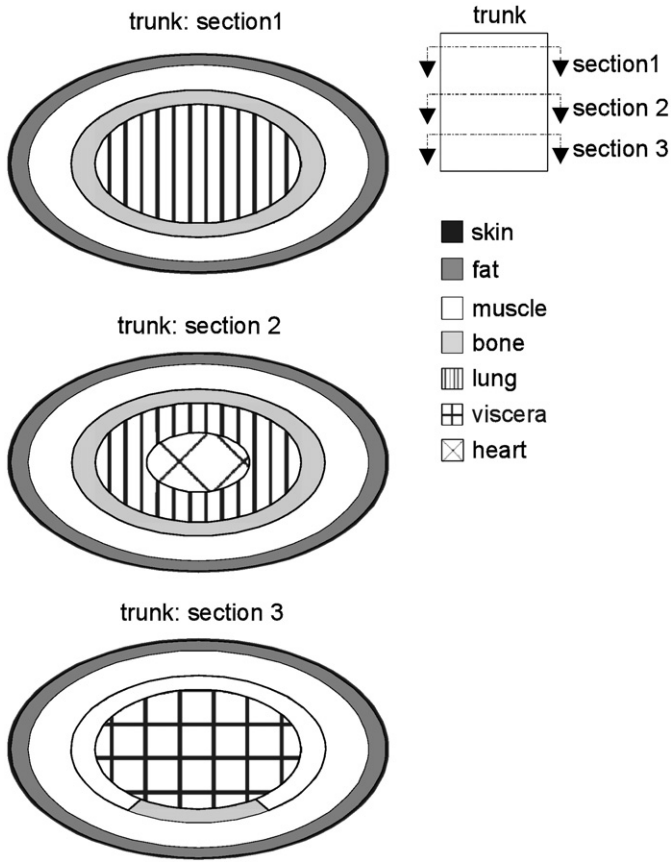


Fig. 3. Distribution of layers in the trunk.

arterial and venous blood flow that enters segment i , $T_{ar,in}$ and $T_{ve,in}$ are the temperature of the arterial and venous blood that enters segment i , $H_{av,i}$ is the heat transfer coefficient between artery and vein reservoirs in segment i .

The blood masses in the reservoirs were calculated considering 5.5 L of blood for a normal adult male with 67 kg [26] and vascular volume data of Chen [24]. The result is presented in Table 4. The heat transfer coefficients between one artery and vein (h_{av}) were calculated using shape factors for two-dimensional conduction between two cylinders immersed in an infinity medium [27]. It is assumed that the artery and vein have the same diameters [27] and the distance between them is given by two times their diameter [28].

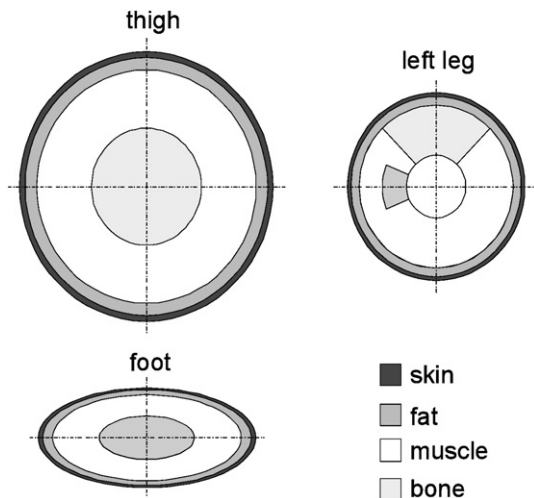


Fig. 4. Distribution of layers in the lower limbs.

Table 3

Convective, radiative, and evaporative heat transfer coefficients used in the model.

Element	Present model		[22]	[23]	
	$\bar{h}_r/$ (W m ⁻² K ⁻¹)	$\bar{h}_c/$ (W m ⁻² K ⁻¹)	$\bar{h}_e/$ (W m ⁻² Pa ⁻¹)	$\bar{h}_c/$ (W m ⁻² K ⁻¹)	$\bar{h}_e/$ (W m ⁻² Pa ⁻¹)
Head	4.1	3.6	5.9	2.7	–
Neck	4.1	3.6	5.9	–	–
Trunk	4.4	3.2	5.3	2.6	4.8
Arm	5.2	2.9	4.8	3.2	–
Forearm	4.9	3.7	6.1	–	6.4
Hand	4.1	4.1	6.8	3.5	–
Thigh	4.3	4.1	6.8	2.9	5.3
Leg	5.3	4.1	6.8	–	–
Foot	3.9	5.1	8.4	–	–
Mean	–	3.3	–	3.2	–

Comparison with experimental data from Nishi and Gagge [22], Kakitsuba and Katsuura [23]. \bar{h}_r , \bar{h}_c and \bar{h}_e are the radiative, convective, and evaporative heat transfer coefficients, respectively.

Multiplying by the number of vessels in one segment, the heat transfer coefficient (H_{av}) for that segment is obtained. The number of vessel pairs per segment is calculated dividing the volume of blood in each element by the volume of each pair (Table 4). The representative diameter of the big arteries and veins adopted was 6 mm. The results are presented in Table 4.

A schematic representation of the passive system model is presented in Fig. 5.

2.4. Thermoregulatory system

The equation used for the vasomotor mechanism was proposed by Savage and Brengelmann [29]:

$$\Delta\omega_{sk} = K_1(T_{hy} - T_{hy,0}) + K_2(T_{sk} - T_{sk,0}) \quad (8)$$

where $\Delta\omega_{sk}$ is the skin blood perfusion rate variation ($814 \times 10^{-6} \leq \Delta\omega_{sk} \leq 3345 \text{ m}^3 \text{ m}^{-3} \text{ s}^{-1}$); K_1 and K_2 are constants, whose values are 1810×10^{-6} and $181 \times 10^{-6} \text{ m}^3 \text{ m}^{-3} \text{ s}^{-1}$, respectively; T_{hy} and $T_{hy,0}$ are the hypothalamus temperature and reference temperature; T_{sk} and $T_{sk,0}$ are the skin and reference temperature.

The equation proposed by Nadel et al. [30] calculates the heat lost by evaporation of sweat:

$$E_{sw,i} = [K_3(T_{hy} - T_{hy,0}) + K_4(T_{sk} - T_{sk,0})] \cdot \exp\left(\frac{T_{sk,i} - T_{sk,0}}{10}\right) \quad (9)$$

where $E_{sw,i}$ is the heat lost by evaporation of sweat in i th segment; K_3 and K_4 are constants, whose values are 197 and $23 \text{ W m}^{-2} \text{ K}^{-1}$. The skin wettedness (w) can be calculated by the equation presented in [21].

Table 4

Volume of blood reservoirs, length, heat transfer coefficients between arteries and veins in each segment.

Element	Arterial		Venous		$h_{av}/$ (W K ⁻¹ pair ⁻¹)	$H_{av}/$ (W K ⁻¹)
	$V_{bi}/$ cm ³	L/cm	Pairs			
Head	40	180	19	–	0	0.00
Neck	15	66	8	16	0.097	1.55
Trunk	446	1484	58	–	0	0.00
Arm	24	107	31	7	0.377	2.55
Forearm	13	60	28	4	0.341	1.43
Hand	7	30	19	3	0.231	0.72
Thigh	78	349	44	15	0.535	8.26
Leg	35	155	40	8	0.487	3.67
Foot	15	66	26	5	0.316	1.55

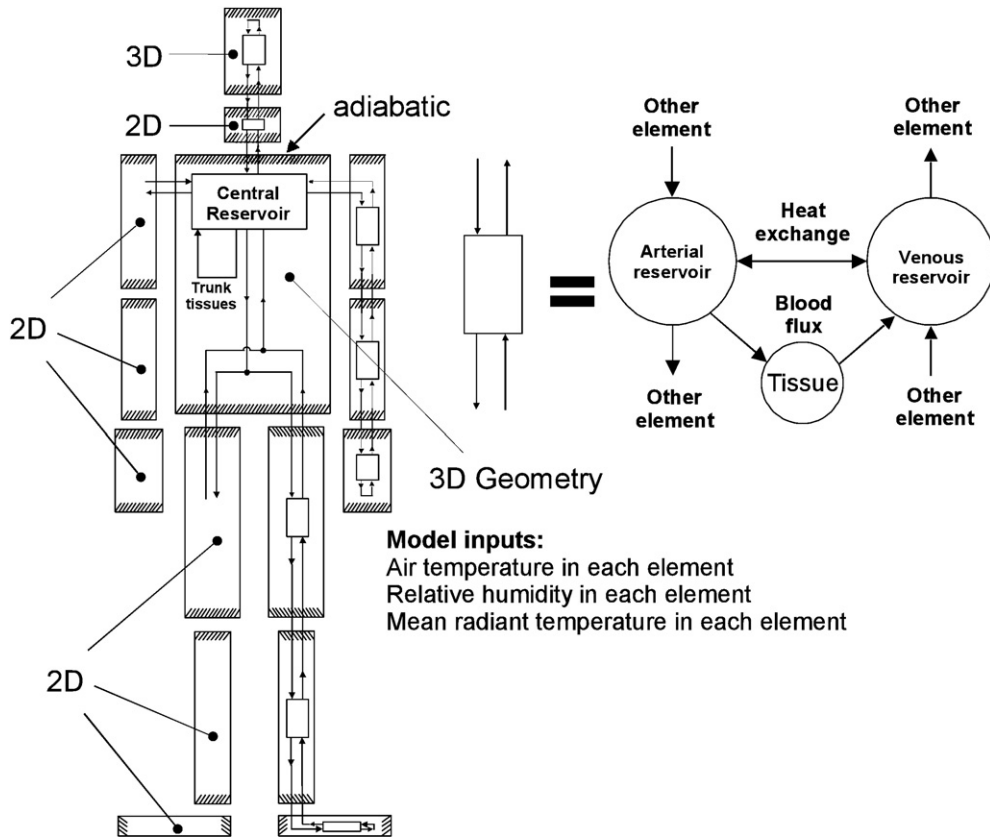


Fig. 5. Overview of the passive system model, showing possible boundary conditions, geometry and circulatory system used in each segment.

Eq. (10) is used to calculate the metabolic heat generation by shivering; it is similar to the equation used by Gordon et al. [6]:

$$M_{sh} \cdot A_s = K_5(T_{hy} - T_{hy,0}) + K_6(T_{sk} - T_{sk,0}) + K_7 \cdot \Delta Q \quad (10)$$

where M_{sh} is the heat generation by shivering ($0 \leq M_{sh} \leq 429$ W, or 6.4 W kg^{-1}), A_s is the superficial area of the model, K_5 , K_6 , and K_7 are constants whose values are 250 W K^{-1} , 40 W K^{-1} , and 0.06 ; ΔQ is the difference between the heat lost in the surface in any instant and the heat lost in thermal neutrality.

2.5. Solution method and computational implementation

The finite-volume method was applied to the differential equations, Eqs. (2), (6), and (7). The resulting algebraic equations were solved by a technique similar to the alternating-direction-implicit scheme [19]. The computer code was written in C++. The use of object-oriented programming produced a computer program that can be easily and quickly modified. It is possible to change the number of elements, layers' distribution, body's constitution, and the number of tissues considered. Several tests were performed in order to evaluate the correctness of the computer implementation and the convergence of the numerical method. A time step of 0.1 s was considered. A grid of $24 \times 20 \times 14$ ($\xi \times \eta \times \gamma$) was used in the head, $24 \times 20 \times 15$ in the trunk,

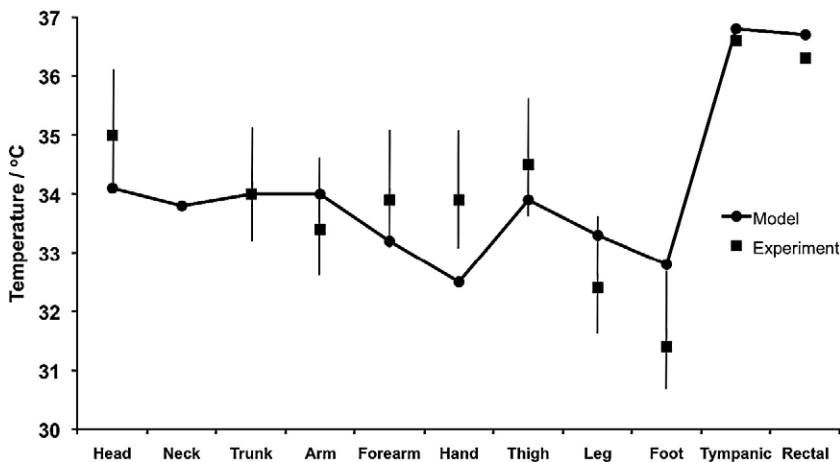


Fig. 6. Predicted values and measured data from [31] at $T_o = 30 \text{ }^\circ\text{C}$, $\phi = 40\%$, and $v < 0.2 \text{ m/s}$.

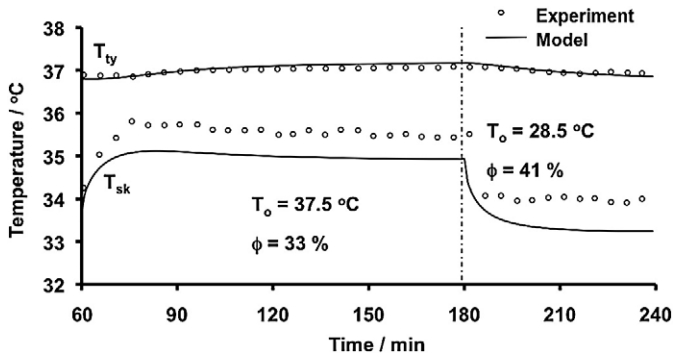


Fig. 7. Predicted values and measured data from Hardy and Stolwijk [33] for hot exposure.

20×20×3 in the other segments. These values are the result of tests performed, allowing a satisfactory volume distribution.

3. Results and discussion

Initially, a steady state simulation was performed in order to determinate the thermal neutrality condition. For normal and nude subjects, the range of operative temperature from 29 to 31 °C provides a thermal neutral condition [21]. In the current model, 30 °C were considered, moreover, $v < 0.15$ m/s, $\phi = 50\%$, and basal conditions were assumed. The nude body model was considered in the stand up position. The viscera and brain mean temperatures can be considered representative of rectal and hypothalamic temperatures, respectively. The mean superficial skin temperature and brain temperatures under this condition serve as set points for the regulatory system. Therefore, the hypothalamic and skin reference temperatures in Eqs. (8)–(10) are 36.8 and 33.7 °C, respectively. Skin superficial and internal temperatures were compared with experimental data from Werner and Reents [31]. The comparison is presented in Fig. 6. In these experiments, air temperature fluctuations along time were of ± 0.2 °C and temporal differences between wall and air temperatures were of ± 1 °C. Considering that a 1 °C increment in operative temperature means approximately 1 °C increase in skin temperature, an accuracy of the measurements of roughly ± 1 °C should be expected. The model is able to predict internal and superficial temperatures with accuracy of less than 1.5 and 4.5%, respectively. The larger differences observed (1.4 °C) were in the extremities, hands and feet. This could be explained by the fact that a simplified circulatory system model was used in these segments. In the feet and hands, there are subcutaneous vascular structures designed for heat transfer [34]. These structures will be included in the future. In addition, it should be necessary to model the fingers, if human thermal responses to extremely cold environment are to be simulated.

The following data result from the choice of the anatomical model. The cardiac output corresponds to the total blood flow that is pumped by the

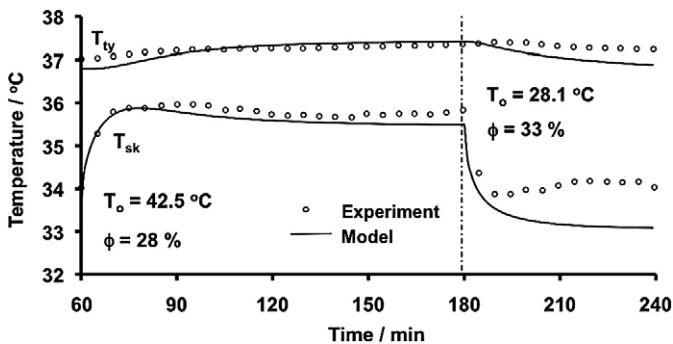


Fig. 8. Predicted values and measured data from Hardy and Stolwijk [33] for hot exposure.

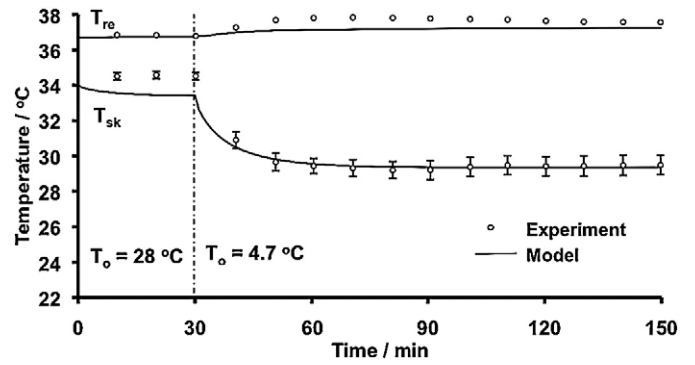


Fig. 9. Model results and measured data presented by Gordon et al. [6] for cold exposure.

heart. A value of 6.2 L/min was calculated at basal condition. This value is superior to the used by Fiala et al. [10] and Al-Othmani et al. [16], 4.9 and 4.8 L/min, respectively. However, it is compatible to the normal cardiac output presented by Aires [32], 3.5 L/(min m²), which corresponds to 6.3 L/min. The basal metabolism calculated was 43.9 W/m², the pulmonary ventilation 6 L/min, and the fat percentage 14%.

In the model, three-dimension geometries were used only in the head and trunk. In the other segments two-dimensional geometries were employed. As expected, the more significant variations occur in the ξ direction. The temperature variations in η direction were smaller than 0.8 °C. The temperature variation in the γ direction of the head was very small and in the trunk it was equal to 0.4 °C.

The comparison between the transient results with reported experimental data from Stolwijk and Hardy [33] can be used to validate the nude body model to a hot exposure. The comparison is presented in Figs. 7 and 8. In these hot-exposure experiments, resting human subjects were exposed consecutively to three different environments. The first exposure lasted 60 min and acted as a preparation period, during which the subjects were exposed to a thermal neutral environment with operative temperatures between 27.8 and 28.5 °C. The objective was to bring the individuals to a condition near thermal neutrality. The second exposure, to a hot environment, lasted 120 min. The third one lasted 60 min. To make possible the comparison between model results and experimental data it was necessary that in both situations the initial point was the same, i.e., 60 min. For the conditions of Fig. 7, the model was able to predict skin and tympanic temperatures with an accuracy of less than 0.8 and 0.2 °C, respectively. For the conditions of Fig. 8, the model was able to predict skin temperature with an accuracy of less than 0.3 °C during the first period (120 min) and 1.0 °C during the last period (120 to 180 min). The tympanic temperature was predicted with an accuracy of less than 0.4 °C during the whole period. A cold exposure simulation was performed and the results were compared with experimental data presented in Gordon et al. [6], see Fig. 9. After 30 min, the difference between the model results and measured values was less than 0.4 °C for the skin, and 0.8 °C for the rectal region.

4. Conclusions

A mathematical model of the human thermal system was successfully developed. The model was built taking into account anthropometrical data, tissues physical properties and physiological parameters of the human body. An anatomic model was adopted and the geometric model constructed using photos of human body cross sections. With the aid of an image editor, it could be concluded that an ellipse was the geometry entity that better represents these cross sections. This way, elliptical cylinders were used to represent the body segments, in contrast with circular cylinders often adopted in similar models. This new technique allowed a more realistic representation of the human body, supporting 3D heat conduction. The anatomic model is composed by 15 cylindrical elements representing the body's segments: head,

neck, trunk, arms, forearms, hands, thighs, legs, and feet. Considering their importance to human regulatory system, 8 types of tissues were considered: skin, fat, muscle, bone, viscera, lung, heart, and brain. These tissues were chosen because they present distinct physical properties and physiological parameters. The heat transfer model considers 3D heat conduction, heat transfer between blood and tissue, heat transfer between large arteries and veins, and heat transfer in the respiratory tract. The model allows the use of different local boundary conditions, but only uniform conditions were employed. The partial differential equations were solved using the finite-volume method. The results of thermal neutrality simulation are in excellent agreement with empirical data, indicating that the model represents satisfactorily the behavior of the passive human thermal system. Although a simplified thermoregulatory model was adopted, the transient results also showed good agreement with experimental data. More comparisons between model results and experimental data are still necessary to validate the clothed model and the asymmetrical environment exposition. The results could be improved by adding more segments: abdomen, fingers and toes, and a more detailed description of the circulatory and thermoregulatory systems. These can be accomplished because of the flexible computational implementation.

References

- [1] P.O. Fanger, Calculation of thermal comfort: introduction of a basic comfort equation, *ASHRAE Transactions* 73 (2) (1967) III.4.1–III.4.20.
- [2] A.P. Gagge, J.A.J. Stolwijk, Y. Nishi, An effective temperature scale based on a simple model of human physiological regulatory response, *ASHRAE Transactions* 77 (1) (1971) 247–262.
- [3] M.S. Ferreira, J.I. Yanagihara, A thermoregulatory model of the human body: exposure to hot environment, *Brazilian Journal of Biomedical Engineering* 15 (1–2) (1999) 87–96.
- [4] E.H. Wissler, Steady-state temperature distribution in man, *Journal of Applied Physiology* 16 (1961) 734–740.
- [5] E.H. Wissler, in: A. Shitzer, R.C. Eberhart (Eds.), *Mathematical Simulation of Human Thermal Behavior Using Whole Body Models*, Heat Transfer in Medicine and Biology, vol. 1, Plenum Press, New York, 1985, pp. 325–373.
- [6] R.G. Gordon, R.B. Roemer, S.M. Horvath, A mathematical model of the human temperature regulatory system – transient cold exposure response, *IEEE Transactions on Biomedical Engineering* 23 (6) (1976) 434–444.
- [7] P. Tikuisis, R.R. Gonzalez, K.B. Pandolf, Thermoregulatory model for immersion of humans in cold water, *Journal of Applied Physiology* 64 (1988) 719–727.
- [8] J. Werner, Man in extreme thermal environment – prediction based on a PC-model, *Journal of Thermal Biology* 18 (1993) 439–441.
- [9] T. Takemori, T. Nakajima, Y. Shoji, A fundamental model of the human thermal system for prediction of thermal comfort, *Transactions of the Japan Society of Mechanical Engineers* 61 (1995) 1513–1520.
- [10] D. Fiala, K.J. Lomas, M. Stohrer, A computer model of human thermoregulation for a wide range of environmental conditions: the passive system, *Journal of Applied Physiology* 87 (1999) 1957–1972.
- [11] D. Fiala, K.J. Lomas, M. Stohrer, Computer predictions of human thermoregulatory and temperature responses to a wide range of environment conditions, *International Journal of Biometeorology* 45 (2001) 143–159.
- [12] C. Huizenga, Z. Hui, E. Arens, A model of human physiology and comfort for assessing complex thermal environments, *Building and Environment* 36 (2001) 691–699.
- [13] S. Tanabe, K. Kobayashi, J. Nakano, Y. Ozeki, M. Konishi, Evaluation of thermal comfort using combined multi-node thermoregulation (65MN) and radiation models and computational fluid dynamics (CFD), *Energy and Buildings* 34 (2002) 637–646.
- [14] M. Salloum, N. Ghaddar, K. Ghali, A new transient bioheat model of the human body and its integration to clothing models, *International Journal of Thermal Sciences* 46 (2007) 371–384.
- [15] X. Wan, J. Fan, A transient thermal model of the human body–clothing–environment system, *Journal of Thermal Biology* 33 (2008) 87–97.
- [16] M. Al-Othmani, N. Ghaddar, K. Ghali, A multi-segmented human bioheat model for transient and asymmetric radiative environments, *International Journal of Heat and Mass Transfer* 51 (23–24) (2008) 5522–5533.
- [17] J. Werner, M. Buse, Temperature profiles with respect to inhomogeneity and geometry of the human body, *Journal of Applied Physiology* 65 (1988) 1110–1118.
- [18] Visible Human Project. Available at Loyola University Chicago home page: <http://meddean.luc.edu/lumen/meded/grossanatomy/cross_section/index>. Access on: march 2000.
- [19] M.S. Ferreira, J.I. Yanagihara, Unsteady heat conduction in 3D elliptical cylinders, *International Communications in Heat and Mass Transfer* 28 (7) (2001) 963–972.
- [20] J.D. Dear, E. Arens, Z. Hui, M. Oguro, Convective and radiative heat transfer coefficients for individual human body segments, *International Journal of Biometeorology* 40 (1997) 141–156.
- [21] ASHRAE: American Society of Heating, Refrigerating and Air-Conditioning Engineers, *Physiological principles and thermal comfort*, in: *Handbook of fundamentals*. Atlanta, 1993, Chapter 8, pp.1–29, Atlanta.
- [22] Y. Nishi, A.P. Gagge, Direct evaluation of convective heat transfer coefficient by naphthalene sublimation, *ASHRAE Transactions* 29 (1970) 830–838.
- [23] N. Kakitsuha, T. Katsura, Direct determination of local evaporative heat transfer coefficient by simultaneous measurement of local sweat rate and evaporation rate, *Journal of the Human-Environment System* 1 (1) (1997) 93–97.
- [24] M.M. Chen, in: A. Shitzer, R.C. Eberhart (Eds.), *The Tissue Energy Balance Equation*, Heat Transfer in Medicine and Biology, vol. 1, Plenum Press, New York, 1985, pp. 153–164.
- [25] H.H. Pennes, Analysis of tissue and arterial blood temperatures in the resting human forearm, *Journal of Applied Physiology* 1 (1948) 93–122.
- [26] A.C. Guyton, *Tratado de fisiologia médica*, Guanabara Koogan, Rio de Janeiro, 1992.
- [27] C.K. Charny, in: Y.I. Cho (Ed.), *Mathematical Models of Bioheat Transfer*, *Advances in Heat Transfer*, vol. 22, Academic Press, San Diego, 1992, pp. 19–155.
- [28] A. Shitzer, L.A. Stroschein, P. Vital, R.R. Gonzalez, K.B. Pandolf, Numerical analysis of an extremity in a cold environment including countercurrent arterio-venous heat exchanges, *Journal of Biomechanical Engineering* 119 (1997) 179–186.
- [29] M.V. Savage, G.L. Bregelmann, Control of skin blood flow in the neutral zone of human body temperature regulation, *Journal of Applied Physiology* 80 (1996) 1249–1257.
- [30] E.R. Nadel, R.W. Bullard, J.A.J. Stolwijk, Importance of skin temperature in the regulation of sweating, *Journal of Applied Physiology* 31 (1971) 80–87.
- [31] J. Werner, T.A. Reents, A contribution to the topography of temperature regulation in man, *European Journal of Applied Physiology* 45 (1980) 95–102.
- [32] M.M. Aires, *Fisiologia*, Guanabara Koogan, Rio de Janeiro, 1992.
- [33] J.A.J. Stolwijk, J.D. Hardy, Partitioned calorimetric studies of responses of man to thermal transients, *Journal of Applied Physiology* 21 (1966) 967–977.
- [34] D.A. Grahn, C.L. Hall, H.C. Heller, Vacuum enhanced heat transfer through mammalian radiator structures, in: *Proceedings of the ASME 2008 Summer Bioengineering Conference (CD)*.